Journal of Applied Electrochemistry **32**: 165–171, 2002.

Electrodeposition of Au–Sn alloys from alkaline baths

B. BOZZINI[1]*, G. GIOVANNELLI[2], S. NATALI[2], M. SERRA[1] and A. FANIGLIULO[1]
[1]*INFM – Dipartimento di Ingegneria dell'Innovazione, Università di Lecce, v. Monteroni, I-73100 Lecce, Italy*
[2]*Dipartimento ICMMPM, Università di Roma 'La Sapienza', v. Eudossiana 18, I-00185 Roma, Italy*
*(*author for correspondence, e-mail: benedetto.bozzini@unile.it)*

Received 26 February 2001; accepted 23 October 2001

Key words: au-sn alloy, white gold, electrodeposition, alkaline baths.

Abstract

A bath for the electrodeposition of white gold alloys of interest for the electroforming of hollow jewellery is proposed. The investigated system is an alkaline $KAu(CN)_2$ bath for the electrodeposition of Au–Sn alloys. The electrochemical investigations are based on cyclic voltammetry and electrodeposition experiments. Electrodeposited foils were studied from the crystallographic, compositional and morphological points of view. Co-deposition of Au and Sn gives rise to the formation of a series of intermetallic phases, which can be detected by X-ray diffraction and anodic stripping. Deposits are typically polyphasic; the phase composition generally does not correspond to the equilibrium one. Chemical compositions ranging from high-Au to high-Sn can be obtained by galvanostatic deposition at suitable current densities.

1. Introduction

A very intriguing, thus far unsolved problem in applied precious-metal electrochemistry, is the electroforming of white alloys. Attempts at plating thick Pt and Au–Ag layers were not successful in practice [1]. The chemistry of Pt baths for the electrodeposition of thick layers is not actually manageable even on a pilot-plant scale. Au–Ag has two major drawbacks: the mechanical properties of the deposits are poor and their colour is exceedingly yellowish, a white metal finish (typically Rh flash) is therefore required and traditional yellow-gold electroforming systems are competitive. Apart from electroforming, as far as thin white precious metal plating is concerned, the commercially viable processes require improvement. The traditional solutions are Rh, Au–Ni and Au–Pd plating. Rh plating is a reliable process; the metal has a perfect white colour but its price has been increasing considerably is the recent past. Au-based alloys are therefore a good alternative. Au–Pd enjoyed considerable attention in the past, but the increase in the price of Pd eventually made the cost of the alloying element higher than that of Au. Au–Ni is the replacement of preference, but well-known allergy problems tend to limit its application as a finishing layer [2]. The field of white metal electroforming and plating therefore appears to be open to innovation.

In this work we propose Au–Sn as an alternative white gold alloy for electrodeposition. An alkaline bath not containing free cyanide is formulated and studied. Particular care is devoted to the determination of the crystalline structure.

The literature on the electrodeposition of Au–Sn alloys is very limited. Three patents on the topic were filed [3]. These texts stress the bath chemistry and the achievable compositional range (high carat alloys), but give no electrochemical or structural details. Recently, the first research paper appeared [4], to the best of the authors' knowledge. This paper provides a rather empirical description of electrodeposition processes from a weakly acidic sulphite bath. Bath preparation is described and some morphological data are reported, but very limited information is given on the electrochemical behaviour. No data are reported on the crystalline structure of the alloys.

2. Experimental

An alkaline Au^+ electrodeposition bath of the following composition was prepared: Au (as $KAu(CN)_2$) 7.5 g l^{-1}, Sn (as $Sn(OH)_6^{2-}$) 75 g l^{-1} and NaOH 80 g l^{-1}. The operating conditions were: current density (c.d.) range 5–50 mA cm^{-2}, T 70 °C.

For cyclic voltammetry (CV) experiments, a 2 M NaOH aqueous solution was used. To this solution $KAu(CN)_2$ and $SnCl_4 \cdot 5H_2O$ were added in order to obtain 10^{-5} and 10^{-4} M solutions of each of the single metals and of both of them.

The electrodeposition set-up for the growth of thick layers (around 50 μm) was a rotating-cathode labora-

tory cell for electroforming. This cell was extensively described in previous work [5, 6]. Instead of cylindrical copper cathodes, in this case square-base prismatic cathodes were used (side: 1 cm, active height 2.5 cm). Two kinds of substrate materials were used: Copper (substrates for high-Au alloys) and Galfan (substrates for low-Au alloys). The substrates were generally dissolved (concentrated HNO_3 for Cu substrates and concentrated HCl for Galfan substrates) in order to obtain four free-standing foils from each electrodeposition run. The homogeneity of the average c.d. distribution and fluid flow, a vital requisite for alloy electrodeposition [1], are ensured in this cell. The cathode rotation rate was 150 rpm, unless otherwise stated.

CV was carried out in a home-made H cell with anodic and cathodic compartments separated by glass frit. The working electrode was an Au wire (diameter 1 mm), after each experiment the working electrode was ground with 1200 and 4000 grit papers and carefully rinsed with distilled water. The counter electrode was a platinum foil (area 3 cm^2). The reference electrode was Ag/AgCl, all voltages are reported vs. Ag/AgCl. The optimal potential scanning rate for the achievement of significant and reproducible voltammetric features was 1 V s^{-1}. A convenient data acquisition rate was 0.5 kHz. The solutions were deaerated with nitrogen and the measurements were carried out under a nitrogen atmosphere. Sets of 60 subsequent potential cycles were recorded. The first cycle showed some easily explained differences (see Section 3.1.) the following ones were practically coincident. Each experiment was repeated several times consecutively and after prolonged (around 8 h) immersion of the electrodes in the solutions. CV experiments were also replicated with different solutions of the same composition, which were prepared independently. No appreciable changes could be measured in both cases.

The crystalline structure of the deposits was analysed by X-ray diffraction with a Cu anticathode and a powder goniometer. The morphology of the deposits was examined by SEM. The composition of the alloys was measured by X-ray fluorescence.

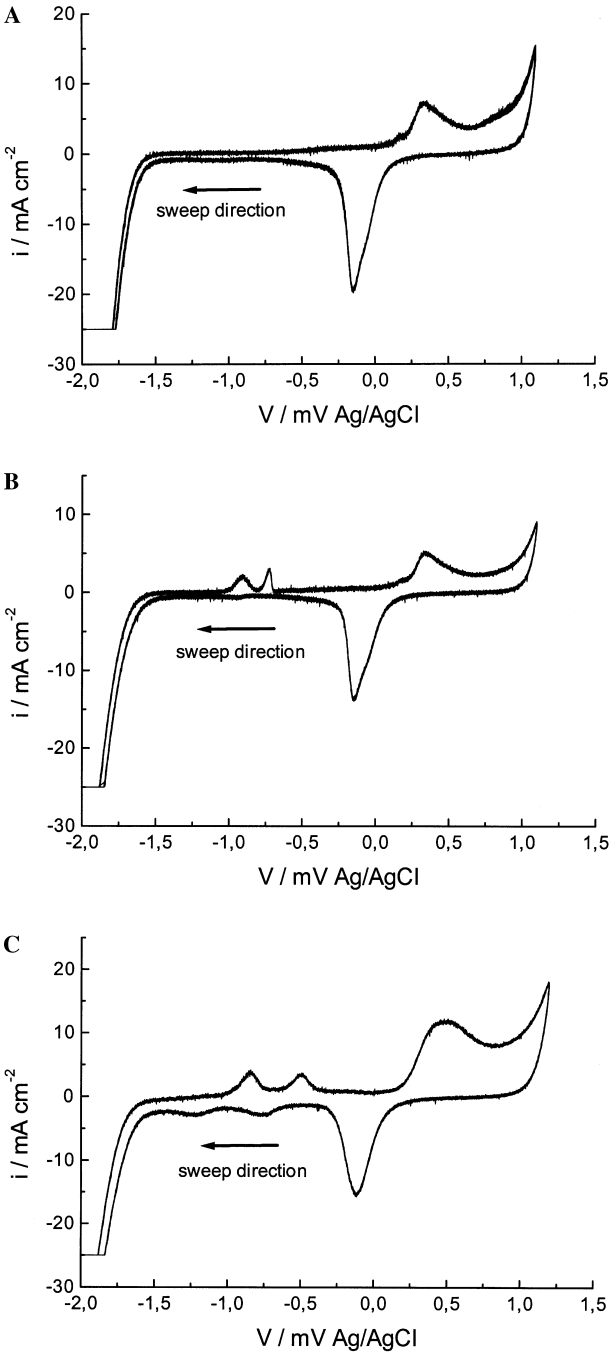

Fig. 1. Cyclic voltammograms (1 V s^{-1}) for polycrystalline Au electrode and solutions: (A) 2 M NaOH, (B) 2 M NaOH + 10^{-5} M $SnCl_4 \cdot 5H_2O$, (C) 2 M NaOH + 10^{-4} M $SnCl_4 \cdot 5H_2O$ + 10^{-5} M $KAu(CN)_2$. Voltammetric scanning range: −2000 to +1100 mV vs. Ag/AgCl.

3. Results and discussion

3.1. *Electrochemical behaviour*

The most typical results of CV investigations are reported in Figures 1–3.

Literature on CV of the Au/Sn system is very limited and focuses on acidic chloride environments [7–9]. In Ref. [7] a UPD peak was observed at approximately −150 mV and two stripping peaks at approximately −140 and +200 mV. The two anodic peaks were assigned to the oxidation of Sn to Sn^{2+} and of Sn^{2+} to Sn^{4+}, respectively. Red-ox reactions undergone by irreversibly adsorbed Sn on poly- and monocrystalline gold substrates were reported in [8, 9]. Sn was adsorbed from a Sn^{2+} aqueous solution. The electrodes were subsequently tested for their red-ox behaviour in $HClO_4$ and H_2SO_4 solutions by CV. In a first anodic process at potentials more negative than approximately +100 mV, the oxidation of Sn does not imply its dissolution and well defined couples of anodic and cathodic peaks were observed. This first process was explained with the formation of oxygenated Sn^{2+} species. Further oxidation (at approximately +200 mV) leads to the dissolution of the adlayer. An exception to this behaviour was noted with Au (1 1 1) substrates, for which the first peak

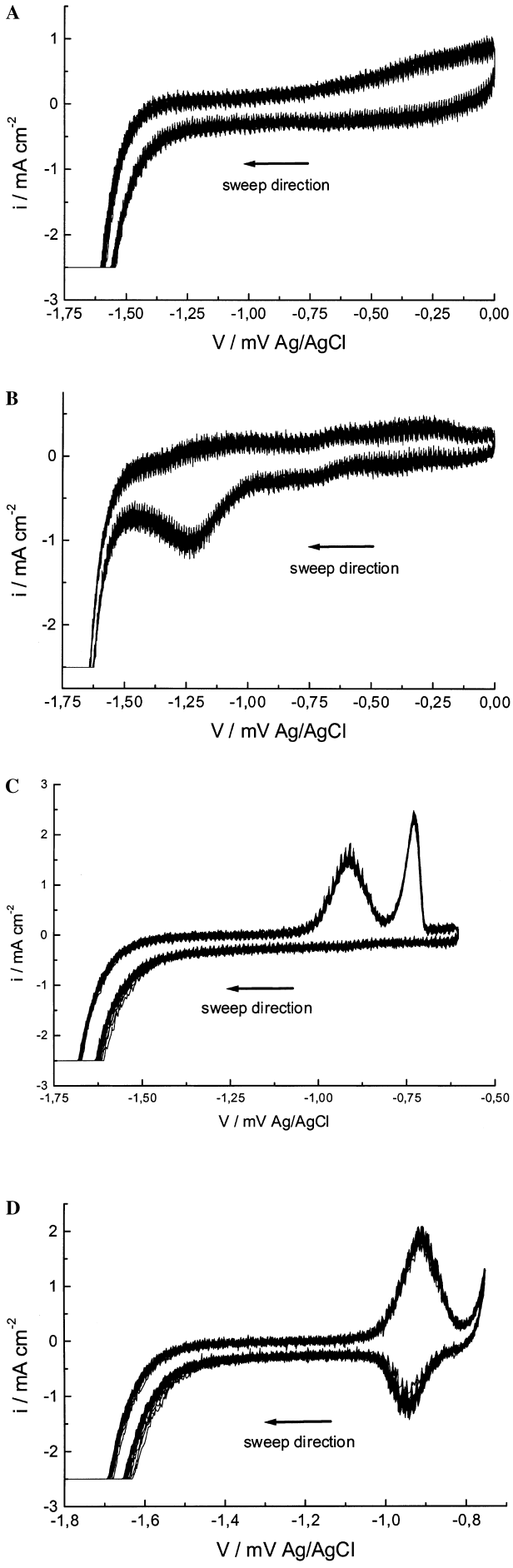

was absent and dissolution of the adlayer occurred in a single step at more positive potentials (>150 mV).

In Figures 1A and 2A we show CVs of the Au electrode in NaOH electrolyte. Oxidation and reduction peaks of Au can be observed at +300 and −100 mV, respectively (Figure 1A). Hydrogen and oxygen evolution features are obvious. The first reduction scan is somewhat different from the subsequent ones and the Au-oxide reduction peak is shifted to less noble potentials. If the cathodic scans are started from −100 mV no Au-oxidation features are noticed (Figure 2A). Hydrogen oxidation at the Au electrode is not observed as a distinct peak.

When $KAu(CN)_2$ is added to the NaOH solution (Figure 2B) a distinct cathodic peak is observed at −1250 mV. The behaviour of the anodic scan is slightly modified by $KAu(CN)_2$ addition, but no peaks can be observed. No effect on the cathodic peak could be observed by changing the $KAu(CN)_2$ concentration from 10^{-5} to 10^{-4} M. This result leads to the conclusion that this peak relates to some sort of pre-deposition and it is possibly correlated with adsorption of a CN^- monolayer and subsequent cathodic passivation; specific SERS investigations are in progress in this group. As previously reported [10] thick Au layers can be deposited from $KAu(CN)_2$ solutions not containing specific additives only within the hydrogen evolution potential region.

When $SnCl_4 \cdot 5H_2O$ is added to the NaOH solution no special cathodic features appear (Figure 2C). The cathodic c.d. rise is delayed by about 150 mV, probably owing to reduction of the electrocatalytic activity by Sn adsorption. Two stripping peaks can be noticed in the anodic scans at −900 and −750 mV, respectively. If Sn^{4+} concentration is increased from 10^{-5} to 10^{-4} M the shape of the stripping peaks is not changed, but their area increases. By analogy with the results of Ref. [9] on stripping of irreversibly adsorbed Sn on Au in acidic solutions, the peak at −900 mV is probably linked to the oxidation of adsorbed species, while the peak at −750 mV is linked to a dissolution reaction. This interpretation is confirmed by reversing the cycle at a potential between the two peaks, which brings about a progressive development of a reversible cathodic peak (Figure 2D). The dissolved species produced at potentials more anodic than −750 mV cannot be reduced at potentials less cathodic than the hydrogen evolution (see Figures 1B and 2C). The presence of Sn in the system does not bring about any alteration of the gold oxidation/reduction features observed at more anodic potentials (Figure 1B).

If both $KAu(CN)_2$ and $SnCl_4 \cdot 5H_2O$ are added (Figures 1C, 2C,D and 3A–C), the voltammetric behaviour of the system depends on the terminal cathodic

Fig. 2. Cyclic voltammograms (1 V s^{-1}) for polycrystalline Au electrode and solutions: (A) 2 M NaOH, (B) 2 M NaOH + 10^{-4} M $KAu(CN)_2$, (C, D) 2 M NaOH + 10^{-5} M $SnCl_4 \cdot 5H_2O$. Voltammetric scanning ranges: (A, B) −2000 to 0 mV vs. Ag/AgCl; (C) −2000 to −550 mV vs. Ag/AgCl; (D) −2000 to −750 mV vs. Ag/AgCl.

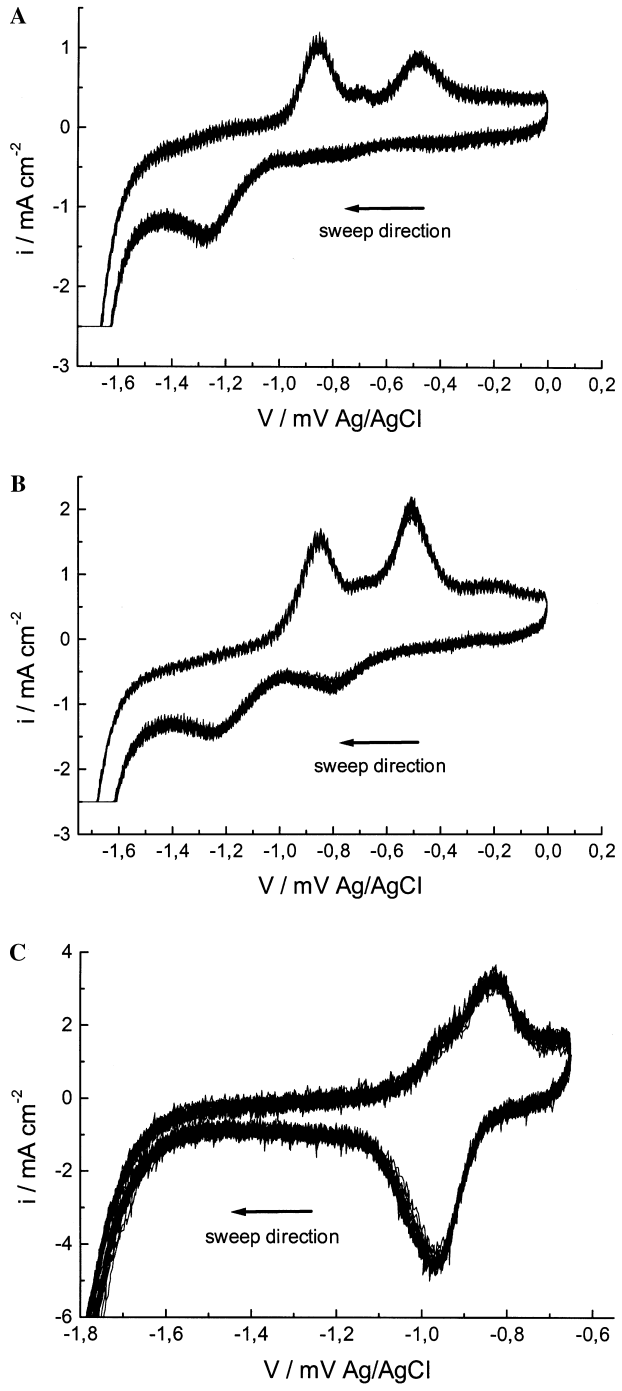

Fig. 3. Cyclic voltammograms (1 V s^{-1}) for polycrystalline Au electrode and solution 2 M NaOH + 10^{-4} M $SnCl_4 \cdot 5H_2O$ + 10^{-5} M $KAu(CN)_2$. A, B, C denote different voltammetric terminal voltages.

voltage. For terminal voltages less cathodic than −1750 mV, the cathodic branch of the curve is the same as observed when only $KAu(CN)_2$ is present (Figure 3A). For cathodic voltages exceeding −1750 mV, a second peak appears at −850 mV (Figure 3B). The anodic branch displays either two or three peaks, two larger ones at −450 and −850 mV and a smaller one at −700 mV (Figure 3A). The anodic peaks appear only for cathodic voltages higher than those corresponding to the peak which develops after addition of $KAu(CN)_2$ (−1250 mV). The appearance of these stripping peaks

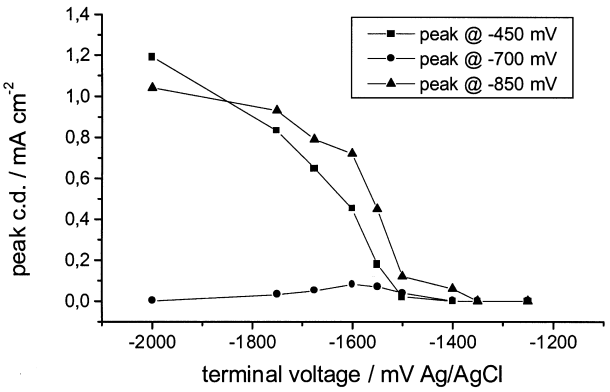

Fig. 4. Stripping peak current densities as a function of cathodic terminal potential from cyclic voltammograms (1 V s^{-1}) for polycrystalline Au electrode and solution 2 M NaOH + 10^{-4} M $SnCl_4 \cdot 5H_2O$ + 10^{-5} M $KAu(CN)_2$.

suggests that co-deposition of Au and Sn starts around −1250 mV. An analysis of the maximum c.d. of the stripping peaks as a function of the terminal cathodic voltage is reported in Figure 4. The peaks at −450 and −850 mV grow with increasing terminal cathodic voltage and their relative intensities reverse. The intensity of the peak at −700 mV goes through a maximum. Even though the stripping peaks which are observed when both $SnCl_4 \cdot 5H_2O$ and $KAu(CN)_2$ are added are shifted with respect to the ones observed when only $SnCl_4 \cdot 5H_2O$ is present and a third weak peak appears, they can still be interpreted in terms of oxidation of insoluble (peak at −850 mV) and soluble (−450 mV) alloy species. As a matter of fact, when the anodic scan is reversed at a potential between the two main stripping peaks, an irreversible cathodic peak develops (see Figure 3C). This peak can be identified with the new cathodic peak which appears when the terminal cathodic voltage exceeds −1750 mV, denoting the formation of a more stable surface alloy. This interpretation is further supported by the alteration of the CV features in the Au-oxidation range (Figure 1C).

From the reported CV plots it can be observed that there is no clear evidence for Sn UPD in this system, even though there is some evidence for the fact that Sn co-deposits with Au at about −1250 mV, more Sn is probably reduced at overpotentials in the hydrogen-reduction potential range. Because of the strong hydrogen-reduction background, it is not easy to extract information about interactions of Au and Sn species from data in this potential range. The lack of variation of the potentials of the Sn-related anodic peaks with terminal cathodic voltage hints at the fact that fixed-stoichiometry alloys are electrodeposited. The variation of the relative intensities of these peaks accounts for a variation of phase composition with co-deposition conditions.

3.2. *Electrodeposition experiments*

Based on CV results, electrodeposition tests were carried out in conditions in which co-deposition of Au and Sn

was anticipated. In order to obtain free-standing foils of thickness ~50 μm, we used a concentrated solution (see Section 2.). Electrodeposition experiments were carried out galvanostatically at a set of c.d.s: 5, 10, 20 and 50 mA cm^{-2}. A rather continuous compositional variation of Au in the range 3–92% is observed. Occasional tests (see separate points in Figure 5) were performed with different rotation rates (100, 150, 250 rpm) and temperatures (50, 70, 85 °C) in order to obtain information of the compositional dependence on these quantities for intermediate Au content alloys (20 mA cm^{-2}). The compositional effects of these variations are compatible with the regular co-deposition behaviour: a decrease in c.d. and increases in temperature and rotation rate correlate with an increase in Au content of the deposits. As previously mentioned, only Au-rich layers were considered in the literature. It is interesting to note that Sn displays a remarkable decolouring effect: only ~8% of Sn is enough to obtain a white alloy.

The morphology of the deposits is smooth for Au-rich layers plated at low c.d.s (Figure 6A, Au 90.5%), while it tends to grow unstable for higher electrodeposition c.d.s (Figure 6B, Au 30.6% and Figure 6C, Au 4.3%). These results are predictable since the strongly complexed Au^+ species tend to yield smooth layers while higher growth rates, achieved with simultaneous hydrogen evolution, are correlated with unstable growth front evolution.

3.3. *Crystallographic structure*

The equilibrium phase structure of the Au–Sn system has been fully characterised previously, the relevant literature is summarised in Ref. [11]. As the Sn content increases, a Au-rich terminal solid solution is followed, at low temperatures, by a series of intermetallics: β-$Au_{10}Sn$ (hexagonal), ζ-(hexagonal) and ζ'-(rhombohedral) Au_5Sn, δ-AuSn (hexagonal), ε-$AuSn_2$ (orthorhombic), η-$AuSn_4$ (orthorhombic) and Sn basically without any solid-state solubility for Au. Powder X-ray diffraction files [12] are available for all these structures and phase assignment in this work was made by comparison with the filed diffraction patterns. The electrodeposited films possess some degree of orientation and, of course, the powder peak intensities do not match those of the films.

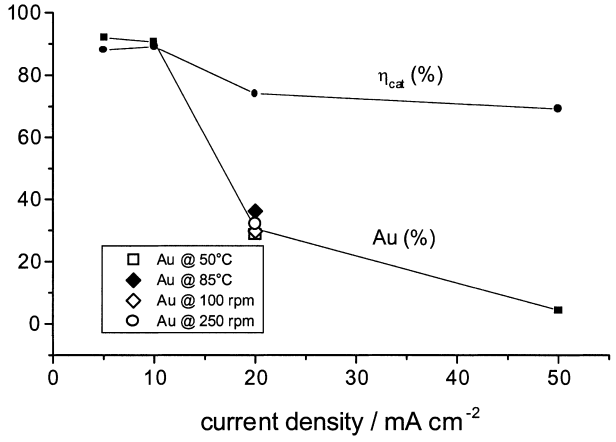

Fig. 5. Composition and current efficiency as a function of electrodeposition current density for the Au–Sn alkaline bath.

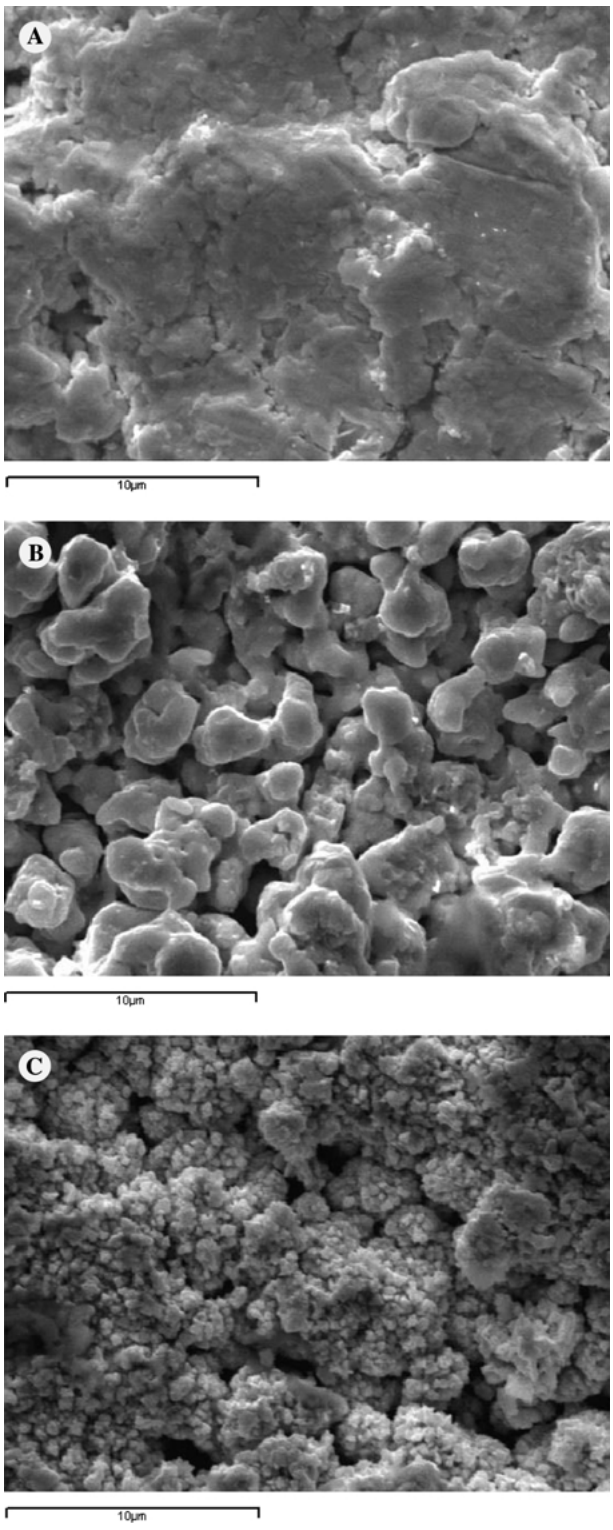

Fig. 6. Surface SEM micrographs of electrodeposits obtained at: (A) 10 mA cm^{-2} (Au 90.5%), (B) 20 mA cm^{-2} (Au 30.6%), (C) 50 mA cm^{-2} (Au 4.3%).

Polyphasic deposits are obtained in the whole investigated c.d. range. It is worth recalling that the polyphasic structure of these electrodeposited alloys is not due to c.d. distribution inhomogeneities, but to the nature of the electrocrystallisation process of this system, as shown in Section 3.1. As a function of galvanostatic deposition conditions different phase compositions were achieved.

(i) 4.3% Au (50 mA cm^{-2}): β-Sn (dominating phase), Au (traces). The equilibrium structure at room temperature is two-phase Sn, ε. A mixed-crystal system containing Au is obtained.

(ii) 30.6% Au (20 mA cm^{-2}) (Figure 7): ε-$AuSn_2$ (dominating phase), δ-AuSn (minority phase), η-$AuSn_4$ (minority phase). The equilibrium structure at room temperature is close to pure η. Again a mixed-crystal deposit is obtained containing the compositionally neighbouring ε-structure together with the δ-structure, which is typical for higher-Au equilibrium systems.

(iii) 90.5% Au (10 mA cm^{-2}) (Figure 8): Au, δ-AuSn. The amount of the two phases is similar. The equilibrium structure at room temperature is two-phase Au, ζ'. A mixed-crystal deposit is obtained containing Au and the neighbouring Sn-richer δ phase.

(iv) 92.0% Au (5 mA cm^{-2}): Au (dominating phase), ζ' (traces) (Figure 9). The two phases present in this structure are the equilibrium ones.

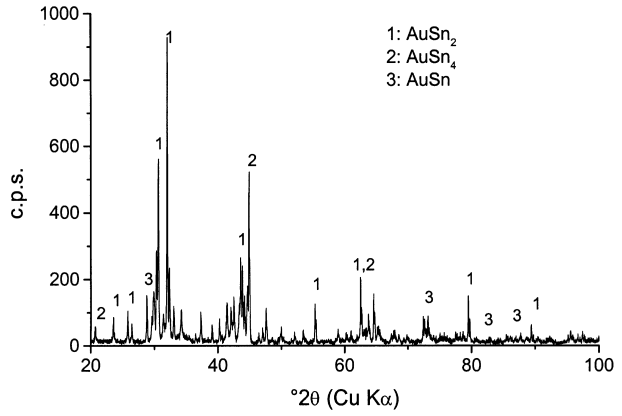

Fig. 7. X-ray diffractogram of a Au–Sn (Au 30.6%) foil electroformed at 20 mA cm^{-2}, for clarity reasons only the main peaks are assigned.

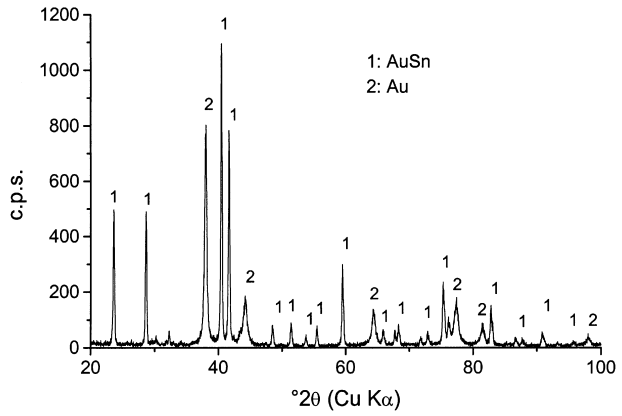

Fig. 8. X-ray diffractogram of a Au–Sn (Au 90.5%) foil electroformed at 10 mA cm^{-2}, for clarity reasons only the main peaks are assigned.

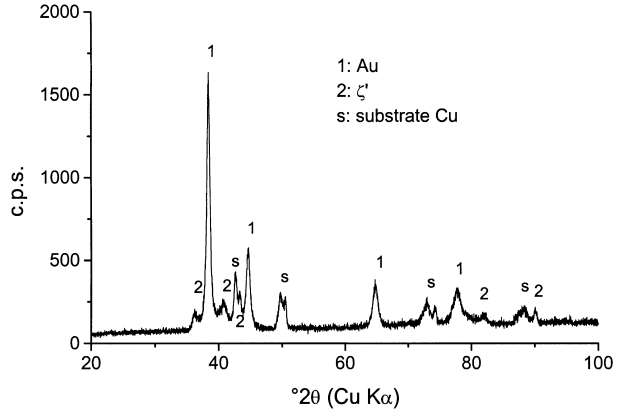

Fig. 9. X-ray diffractogram of a Au–Sn (Au 92%) electrodeposit at 5 mA cm^{-2}.

The tendency for the formation of intermetallic phases can be correlated with the formation of well-defined anodic peaks observed in CV tests, even though a one-to-one correspondence cannot be established on the basis of the present data. The study of the anodic behaviour of well-defined single phase materials, the preparation of which is in progress, will provide conclusive evidence on the correlation between crystalline structure and voltammetric stripping behaviour.

4. Conclusions

As far as composition and phase structure of electrodeposited gold-alloys are concerned, UPD effects are known to be very important for the electrodepostion of Au–Cu, Au–Cu–Cd, Au–Cd and Au–Tl. In the alkaline Au–Sn system studied in this work UPD behaviour is not obvious and fixed stoichiometries in extended c.d. ranges and one-phase deposits cannot be easily obtained. Nevertheless, some subtler form of cathodic interaction of the two metals is probably present giving rise to the formation of several intermetallic phases. This was proved directly by X-ray diffractometry and indirectly by anodic stripping voltammetry. Electrodeposited Au–Sn alloys from the investigated alkaline bath are typically polyphasic, the phase composition is generally not the equilibrium one. Free-standing objects of white Au alloys of perspective interest for the electroforming of hollow jewellery can be obtained from the proposed alkaline bath.

References

1. B. Bozzini and P.L. Cavallotti, *Trans. IMF* **78** (2000) 227.
2. P. Bagnoud, S. Nicoud and P. Ramoni, *Gold Technology* **18** (1996) 11.

3. W. Zilske, Electrolytic bath and process for the deposition of gold alloy coatings, US Patent 4 391 679; P. Stevens, Tin–Gold electroplating bath and process, US Patent 4 013 523; F. Zantini, Electrodeposition of gold alloys, US Patent 3 764 489.
4. W. Sun and D.G. Ivey, *Mat. Sci. Eng*. **B65** (1999) 111.
5. B. Bozzini, G. Giovannelli and P.L. Cavallotti, *J. Appl. Electrochem*. **29** (1999) 685.
6. B. Bozzini, G. Giovannelli and P.L. Cavallotti, *J. Appl. Electrochem*. **30** (2000) 591.
7. V.A. Vicente and S. Bruckenstein, *Anal. Chem*. **44** (1972) 297.
8. A. Rodes, J.M. Feliu, A. Aldaz and J. Clavilier, *J. Electroanal. Chem*. **256** (1988) 455.
9. A. Rodes, E. Herrero, J.M. Feliu and A. Aldaz, *J. Chem. Soc., Faraday Trans*. **92** (1996) 3769.
10. B. Bozzini, P.L. Cavallotti, G. Giovannelli and S. Natali. In '*Hydrogen at Surfaces and Interfaces*', G. Jerkiewicz, J.M. Feliu, B.N. Popov (eds), Proc. 197th ECS Meeting, Toronto, Canada,14–18/05/2000, PV 2000-16 Electrochemical Society Proceedings, p.242.
11. D. Okamoto and T.B. Massalski, 'Phase Diagrams of Binary Gold Alloys', Binary Alloy Phase Diagram Monograph Series (ASM International, 1987).
12. JCPDS 'Powder Diffraction Files,' International Centre for Diffraction Data, Newtown Square, PA, USA.